Double Recycled radiopulsars: The Best Gravitational Laboratory.

G.S.Bisnovatyi-Kogan (IKI, Moscow)

1. Pulsars and close binaries
2. Hulse-Taylor pulsar
3. Disrupted pulsar pairs
4. RP statistics
5. Enhanced evaporation: formation of single RP
6. GR Effects: NS+NS
7. A Double-Pulsar System
8. Checking General Gelativity
9. Past and Future of PSR J0737-3039A,B
10. Variability of the gravitational constant.

MEPhI School, 31 May, 2006

Discovery of pulsars: A.Hewish, J.Bell et al., 1968, Nature, **217**, 709

1973: all pulsars are single (more than 100)

more than half massive stars (predesessors of pulsars) are in binaries.

Possible explanations: pair disruption during explosion

no possibility to form a radiopulsar in pairs

1971: X-ray satellite UHURU

Discovery of X-ray pulsars in binaries.

Her X-1: **X ray** pulsar

Period of pulsations P(p)=1.24 sec, orbital P(orb)=1.7 days

Neutron star mass 1.4 Solar masses

Optical star mass about 2 Solar masses

This system should give birth to the binary radiopulsar

Bisnovatyi-Kogan G.S. and Komberg B.V., 1974, Astron. Zh. **51**,373

Reasons:

1. After 100 million years the optical star will become a white dwarf, mass transfer will be finished, and the system will be transparant to radio emission.

2. X ray pulsar is accelerating its rotation due to accretion, so after the birth of the white dwarf companion the neurton star will rotate rapidly, P(p) about 100 msec.

Question:

Why are the binary radiopulsars not found (1973) ?

Answer (B-K, K, 1974):

Because the magnetic field of the neutron star is decreasing about 100 times during the accretion, so binary radiopulsars are very faint objects,

Pulsar luminosity $L \sim B^2/P^4$

At small B luminosity L is low even at the rapid rotation

Magnetic field is screened by the infalling plasma

Pulsars and close binary systems

G. S. Bisnovatyi-Kogan and B. V. Komberg

Institute of Applied Mathematics,
Academy of Sciences of the USSR
(Submitted April 27, 1973)
Astron. Zh., 51, 373-381 (March-April 1974)

The absence of radio pulsars from binary systems might be attributable to a decay in the magnetic field of a neutron-star binary component as accretes material from the primary star. Thus even after accretion ceases and radio waves are no longer absorbed, the neutron-star component would not be observable as a radio pulsar. An analysis of the accelerated rotation of the x-ray pulsar Her X-1, which belongs to a close binary, also implies a weaker magnetic field ($B \leqslant 10^{10}$ gauss) than in radio pulsars. The evolution of a close binary whose components have nearly equal masses is considered qualitatively. The more massive star may be the first to explode as a supernova, followed by disruption of the binary system. Soon the companion should also explode as the two stars will have evolved concurrently. This situation could produce a pair of radio pulsars located close together. The space distribution of radio pulsars is examined; several pairs of nearby pulsars at high galactic latitudes are identified. An observational test is proposed for the hypothesis that such pairs originate from the disruption of a binary: The magnitude and direction of their peculiar velocity would be measured.

We therefore see that evolutionary considerations certainly do not preclude the possibility that a neutron star might be found paired with another star also in a terminal evolutionary stage (white dwarf, neutron star, "collapsar"); on the contrary, they point to such a conclusion with high probability. Hence the absence of radio pulsars from close binary systems requires, as we have indicated at the beginning of Sec. 3, a further assumption regarding the decay of the magnetic field.

DISCOVERY OF A PULSAR IN A BINARY SYSTEM

R. A. HULSE AND J. H. TAYLOR

THE ASTROPHYSICAL JOURNAL, **195**:L51–L53, 1975 January 15

Received 1974 October 18

PARAMETERS OF THE BINARY PULSAR

$\alpha(1950.0)$	$= 19^h13^m13^s \pm 4^s$
$\delta(1950.0)$	$= +16°00'24'' \pm 60''$
l	$= 49.°9$
b	$= 2.°1$
P_{cm}	$= 0.^s059030 \pm 0.^s000001$
dP_{cm}/dt	$< 1 \times 10^{-12}$
DM	$= 167 \pm 5$ cm^{-3} pc
S_{430}	$= 0.006 \pm 0.003$ Jy
W_e	< 10 ms

ELEMENTS OF THE ORBIT

K_1	$= 199 \pm 5$ km s^{-1}
P_b	$= 27908 \pm 7$ s
e	$= 0.615 \pm 0.010$
ω	$= 179° \pm 1°$
T	$=$ JD 2,442,321.433 $\pm$ 0.002
$a_1 \sin i$	$= 1.00 \pm 0.02\ R_\odot$
$f(m)$	$= 0.13 \pm 0.01\ M_\odot$

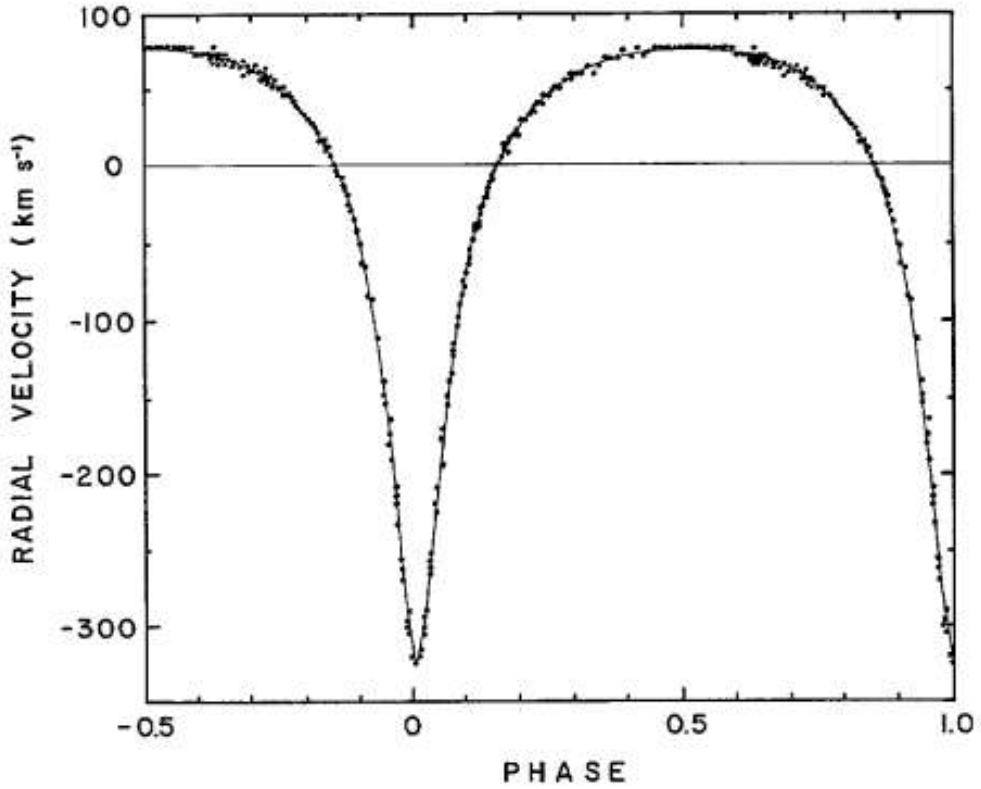

FIG. 1.—Velocity curve for the binary pulsar. Points represent measurements of the pulsar period distributed over parts of 10 different orbital periods. The curve corresponds to equations (1)–(4), with parameters from table 2.

Physics Today
1975, 28, No.11,
pp. 46-54

Informal discussion
at Landau Theor. Inst.

Left to right:

G.S.Bisnovatyi-Kogan,
I.D.Novikov,
Academicians
V.L.Ginzburg and
Ya.B.Zeldovich, and
David Pines.
(Photo G.Baym)

The properties of the first binary pulsar coinside with our predictions:
Rapid rotation and **Small magnetic field**

Possible evolution of a binary-system radio pulsar as an old object with a weak magnetic field

G. S. Bisnovatyi-Kogan and B. V. Komberg

Pis'ma Astron. Zh. 2, 338–342 (July 1976)

Taylor et al.[3] have recently reported measurements of $\dot{P}_{rot}$ for PSR 1913 + 16, which has the anomalously small value $\dot{P}_{rot} = (8.8 \pm 0.3) \cdot 10^{-18}$ for its value of P_{rot}. Knowing $\dot{P}_{rot}$ for PSR 1913 + 16, we can readily estimate its rate of rotational-energy loss,

$$\dot{E} = -I\Omega\dot{\Omega} = I\left(\frac{2\pi}{P_{rot}}\right)^2 \frac{\dot{P}_{rot}}{P_{rot}} = 2 \cdot 10^{33} \text{ erg/sec},$$

$$B_s = \left(\frac{3Ic^3 P_{rot}\dot{P}_{rot}}{8\pi^2 R_{NS}^6}\right)^{1/2} \approx 2.3 \cdot 10^{10} \text{ gauss},$$

The average magnetic fields of single radiopulsars is about 10^{12} Gauss.

Single pulsars of common origin (B-K, K (1974)

TABLE 1. Possible Pairs of Pulsars

Pair No.	Designations	Positions				P, sec	Disp. measure, pc/cm³	$\dot{P}$, 10^{-9} sec/day	$\tau = \frac{P}{\dot{P}}$, yr
		R. A.	Decl.	l^{II}	b^{II}				
1	P 0943+10	$9^h43^m20^s$	10°05′33″	225.4	43.2	1.098	15	—	—
	P 0950+08	9 50 31	08 09 43	228.[illegible]	43.7	0.253	3	0.0198	$3.5 \cdot 10^7$
2	P 0809+74	8 09 03	74 38 10	14[illegible]	31.6	1.30	6	0.014	$2.5 \cdot 10^8$
	P 0904+77	9 04	77 40	135.3	33.7	1.58	—	—	—
3	P 1700—18	17 00 56	—18	4.0	14.0	0.802	<40	0.154	$6.9 \cdot 10^8$
	P 1706—16	17 06 33	—16 37 21	5.8	13.7	0.653	25	0.55	$3.3 \cdot 10^8$
4	P 0329+54	3 29 11	54 24 38	145.0	—1.2	0.714	27	0.177	$1.1 \cdot 10^7$
	P 0355+54	3 55 00	54 13	148.1	0.9	0.156	55	—	—
5	P 0525+21	5 25 45	21 55 32	183.8	—6.9	3.7455	51	3.452	$3 \cdot 10^8$
	P 0531+21	5 31 31	21 56 55	184.6	—5.8	0.03313	57	36.526	$2.5 \cdot 10^8$
6	P 1426—66	14 26 34	—66 09 94	312.3	—6.3	0.787	60	—	—
	P 1449—65	14 49 22	—65	315.3	—5.3	0.180	90	—	—
7	P 1845—01	18 45	—01 27	31.3	0.2	0.660	90	—	—
	P 1845—04	18 45 10	—04 05 32	28.9	—1.0	0.598	142	—	—
8	P 2016+28	20 16 00	28 30 31	68.1	—4.0	0.558	14.16	0.01	$1.2 \cdot 10^8$
	P 2020+28	20 20 33	28 44 30	68.9	—4.7	0.343	—	—	—
9	P 2111+46	21 11 41	46 36	89.1	—1.2	1.015	141.4	—	—
	P 2154+40	21 54 56	40 00	90.5	—11.5	1.525	110	—	—
10	P 0611+22	6 11 10	22 35	188.7	2.4	0.335	99	—	—
	P 0540+23	05 40 10	23 30	184.4	—3.3	0.246	72	—	—

Pulsar Astrometry at the Microarcsecond Level

Mem. S.A.It. Vol. 75, 282

W.H.T. Vlemmings[1], S. Chatterjee[2], W.F. Brisken[3]

et al.

Separated at birth: B2021+51 and B2020+28

2020+28

2016+28 **B-K, K (1974)**

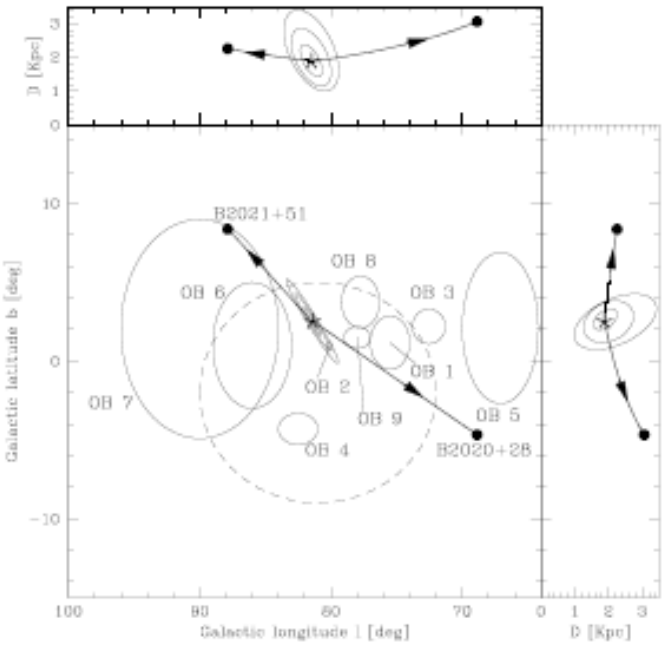

Fig. 2. The 3-dimensional pulsar motion through the Galactic potential for B2020+28 and B2021+51. The dashed circle represents the Cygnus superbubble, while the labelled solid ellipses are the Cygnus OB associations with positions and extents as tabulated by Uyaniker et al. (2001). The extent of OB 2 is unknown and only the centre of the association is indicated. The thick solid lines indicate the pulsar paths, with the origin denoted by the starred symbol and the arrows pointing in the direction of motion. The current positions are indicated by the solid dots. The elliptical contours around the pulsars' origin in these panels indicate the 1, 2 and 3σ levels of the likelihood solution for the birth location.

2006: New class of neutron stars: recycled pulsars, more than 180 objects.

All passed the stage of accreting pulsars, accelerating the rotation and decreasing the magnetic field.

Ordinary pulsars	Recycled pulsars
P=0.033 – 8 sec	P=1.5 – 50 msec
B= 10^{11} - 10^{13} Gauss	B=10^{8} - 10^{10} Gauss

The ubiquitous $P - \dot{P}$ diagram shown for a sample of radio pulsars. Those objects known to be members of binary systems are highlighted by a circle (for low-eccentricity orbits) or an ellipse (for elliptical orbits). Pulsars thought to be associated with supernova remnants are highlighted by the starred symbols, from

Lorimer (2001) astro/ph-0104388

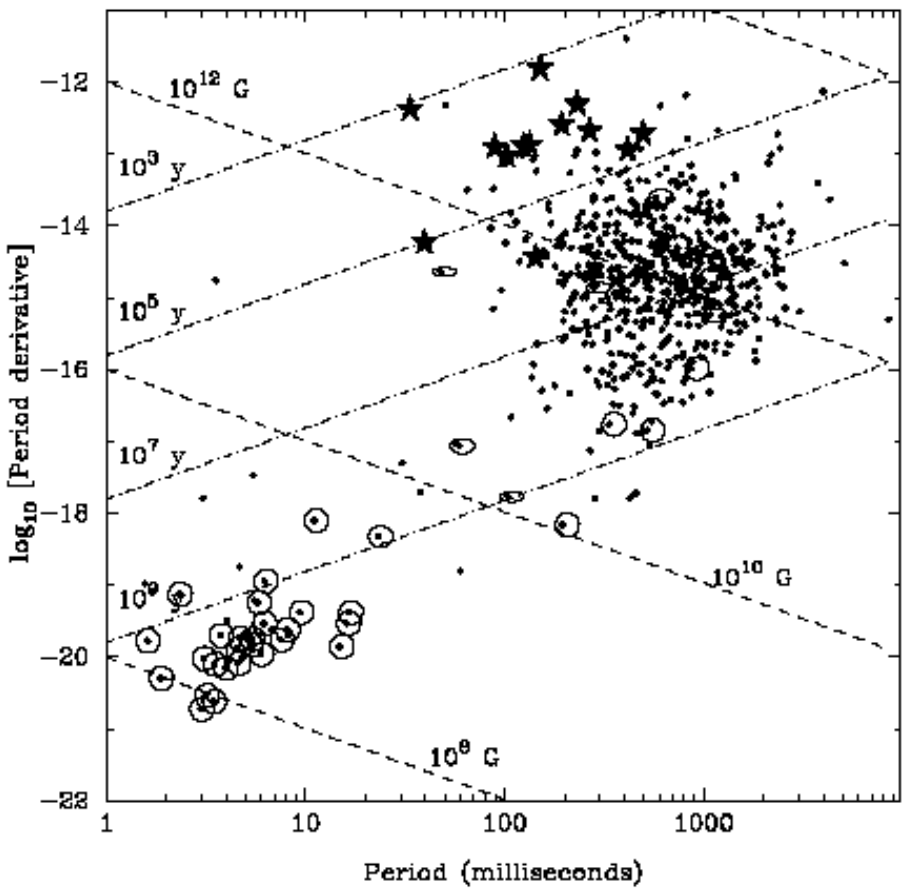

Рис. 1: Диаграмма распределения радиопульсаров на плоскости $P - \dot{P}$ (период - производная периода). Точки, соответствующие объектам в двойных системах, обведены кружочками для орбит с малым эксцентриситетом, и эллипсами для эллиптических орбит. Пульсары, подозреваемые в связи с остатками сверхновых, отмечены звездочками; из [65]

Recycled pulsars: NS + WD and single - about 180 objects

NS + NS 6 objects (like Hulse- Taylor pulsar)

Single recycled pulsars (small P and B) passed the stage of X-ray pulsar in binary, and later had lost the companion WD.

NS + NS are in the Galaxy disk

NS + WD and single are in the galactic bulge, and in the globular clusters.

Globular clusters contain 0.001 of the mass of the Galaxy, and about ½ of the recycled pulsars.

Formation of the binary in GC by tidal capture or triple colllision

Disruption of the binary RP by collisions with GC stars: most single RP are situated in GC.

31 RP in Terzian 5 (11 – BP, 10 +10? – single)

22 RP in 47 Tuc (14 – BP, 7 + 1? – single)

In total: 80 RP in Gal (15 – single), 108 RP in GC (40+15? – single)

Disruption of binary by close stellar encounters

Hard pairs become harder, soft pairs become softer

V(star, pair)>V(star, field) – hard pair.
V(star, pair)<V(star, field) – soft pair.

One of the component in binary (degenerate dwarf) fills its Roche Lobe

R(dwarf) increases with decreasing mass
R(Roche lobe) = R(dwarf)

The pairs with RP are hard.

Loosing angular momentum by a hard pair due to encounters make the pair softer, if the dwarf fills its Roche Lobe, due to enhanced overflowing, similar to gravitational wave emission

Finally the encounters disrupt the binary in Globular Clusters during t<t(Galaxy life time).

Enhanced evaporation

Bisnovatyi-Kogan, Astrofizika, 32, 313 (1990)

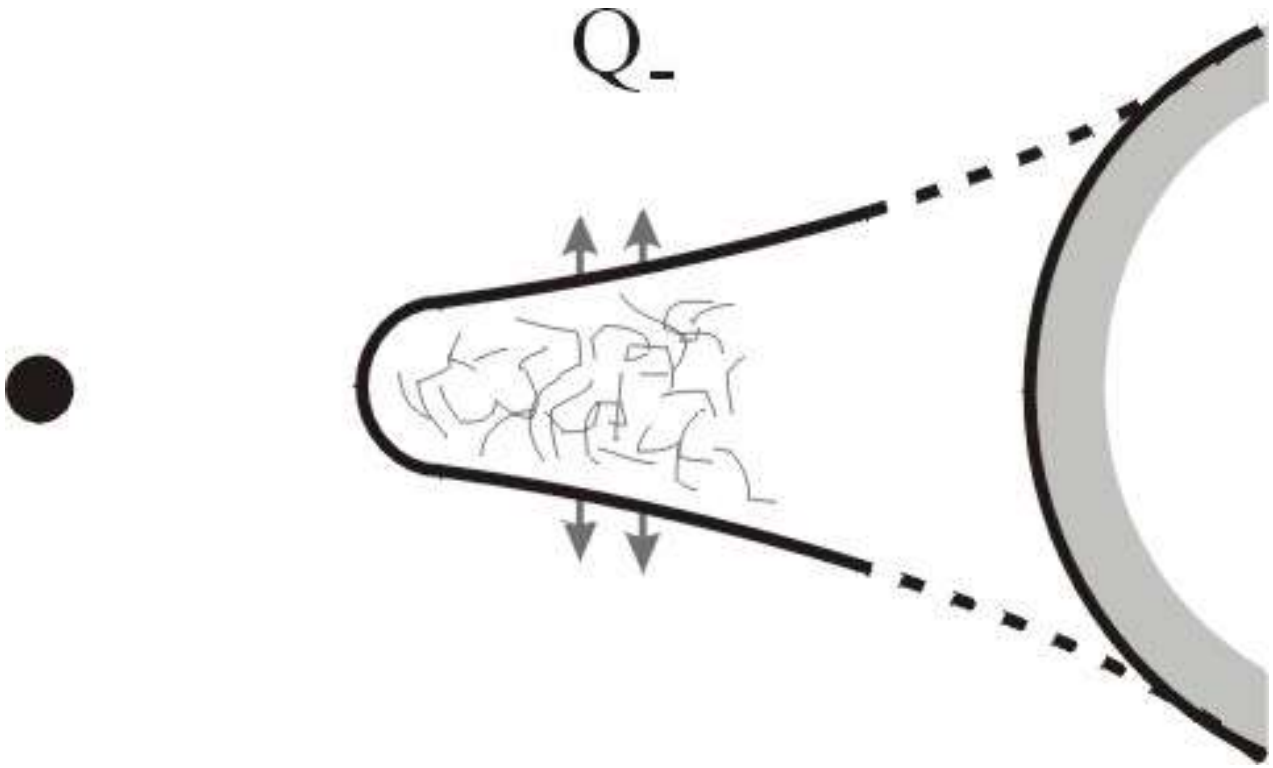

GR Effects:

NS+NS

$$\dot{\omega} = 3T_{\odot}^{2/3} \left(\frac{P_b}{2\pi}\right)^{-5/3} \frac{1}{1-e^2} (M_A + M_B)^{2/3},$$

$$\gamma = T_{\odot}^{2/3} \left(\frac{P_b}{2\pi}\right)^{1/3} e \frac{M_B(M_A + 2M_B)}{(M_A + M_B)^{4/3}},$$

$$\dot{P}_b = -\frac{192\pi}{5} T_{\odot}^{5/3} \left(\frac{P_b}{2\pi}\right)^{-5/3} \frac{\left(1 + \frac{73}{24}e^2 + \frac{37}{96}e^4\right)}{(1-e^2)^{7/2}} \frac{M_A M_B}{(M_A + M_B)^{1/3}},$$

$$r = T_{\odot} M_B,$$

$$s = T_{\odot}^{-1/3} \left(\frac{P_b}{2\pi}\right)^{-2/3} x \frac{(M_A + M_B)^{2/3}}{M_B},$$

$$T_{\odot} = GM_{\odot}/c^3 = 4.925490947 \mu c,$$

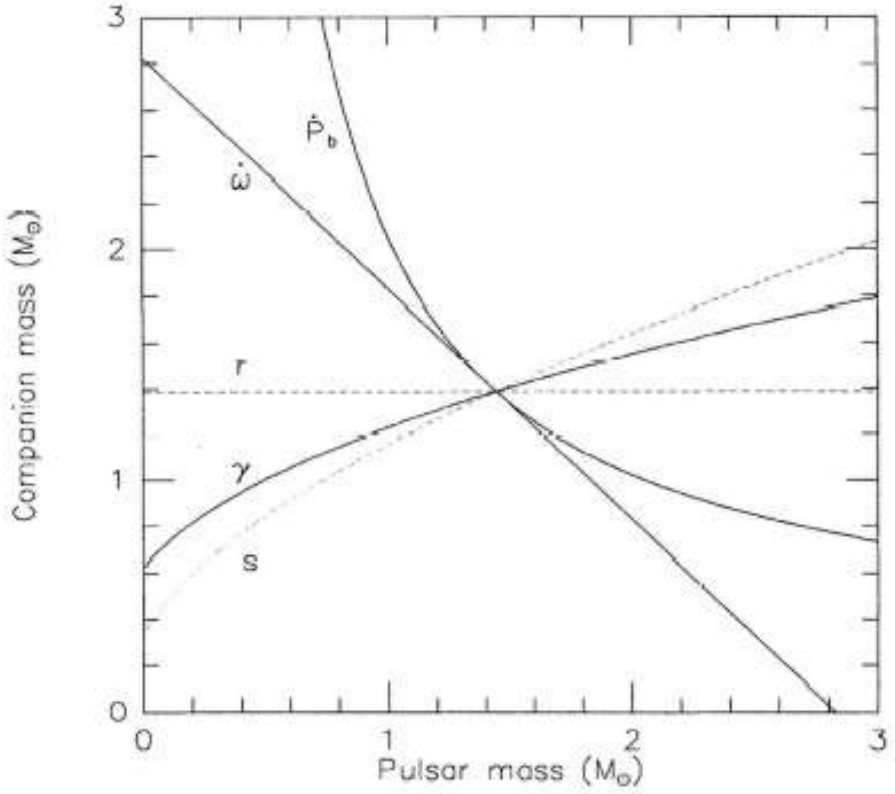

Рис. 2: Сплошные кривые соответствуют уравнениям (14-16) при учете измеренных значений $\dot{\omega}$, γ и $\dot{P}_b$. Пересечения этих кривых в одной точке (в пределах экспериментальной неопределенности порядка 0.35% в $\dot{P}_b$) устанавливает существование гравитационных волн. Штриховые линии соответствуют *предсказанным* значениям параметров r и s. Эти значения могут стать измеримыми при дальнейшем улучшении качества данных, из [96].

NS + NS RP are the best laboratories for checking of General Relativity
1913+16 timing had shown (indirectly) the existence of gravitational waves
Nobel Prize of Hulse and Taylor (1993)

A Double-Pulsar System — A Rare Laboratory for Relativistic Gravity and Plasma Physics (Lyne et al., 2004)

The clock-like properties of pulsars moving in the gravitational fields of their unseen neutron-star companions have allowed unique tests of general relativity and provided evidence for gravitational radiation. We report here the detection of the 2.8-sec pulsar J0737-3039B as the companion to the 23-ms

pulsar J0737-3039A in a highly-relativistic double-neutron-star system, allowing unprecedented tests of fundamental gravitational physics. We observe a short eclipse of J0737-3039A by J0737-3039B and orbital modulation of the flux density and pulse shape of J0737-3039B, probably due to the influence of J0737-3039A's energy flux upon its magnetosphere. These effects will allow us to probe magneto-ionic properties of a pulsar magnetosphere.

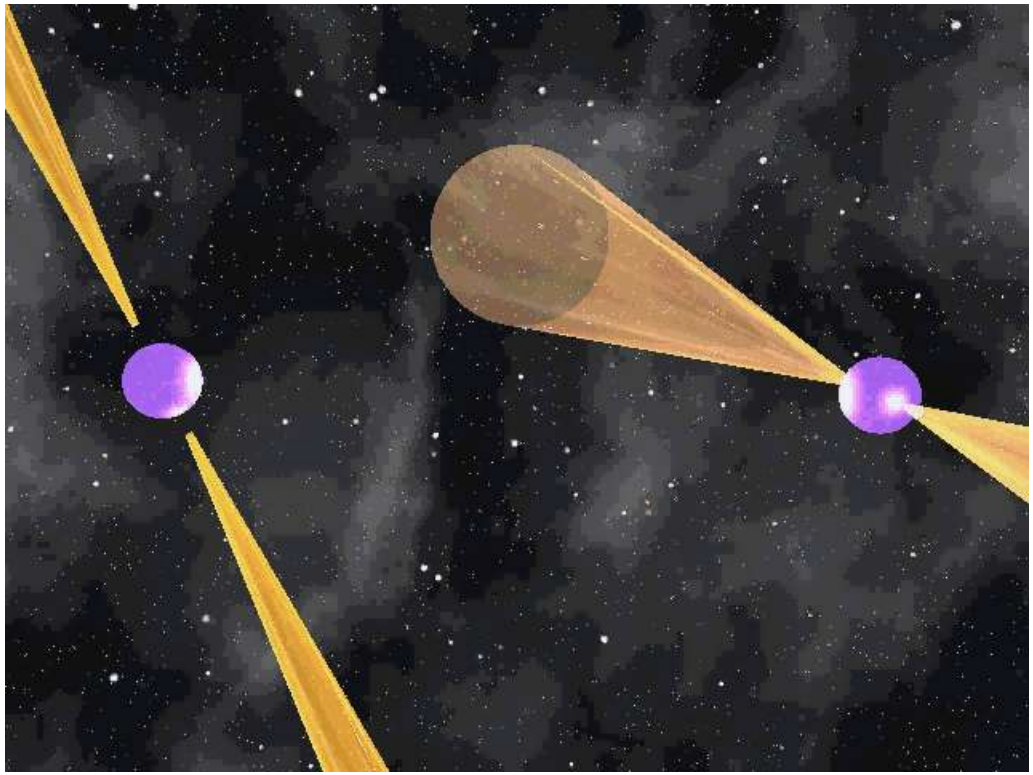

Table 1: Observed and derived parameters of PSRs J0737−3039A and B using the DD timing model (*11, 13*). Standard ($1\,\sigma$) errors are given in parentheses after the values and are in units of the least significant digit(s). The parameters A, B and δ_r in the DD model were assumed to be zero in the analysis. The distance is estimated from the dispersion measure and a model for the interstellar free electron distribution (*32*).

Pulsar	PSR J0737−3039A	PSR J0737−3039B
Pulse period P (ms)	22.69937855615(6)	2773.4607474(4)
Period derivative $\dot{P}$	$1.74(5) \times 10^{-18}$	$0.88(13) \times 10^{-15}$
Epoch of period (MJD)	52870.0	52870.0
Orbital period $P_{\rm b}$ (day)	0.102251563(1)	–
Eccentricity e	0.087779(5)	–
Epoch of periastron T_0 (MJD)	52870.0120589(6)	–
Longitude of periastron ω (deg)	73.805(3)	73.805 + 180.0
Projected semi-major axis $x = a \sin i/c$ (sec)	1.41504(2)	1.513(4)
Advance of periastron $\dot{\omega}$ (deg/yr)	16.90(1)	–
Gravitational redshift parameter γ (ms)	0.38(5)	
Shapiro delay parameter s	$0.9995(-32, +4)$	
Shapiro delay parameter r (μs)	$5.6(-12, +18)$	

Characteristic age τ (My)	210	50
Surface magnetic field strength B (Gauss)	6.3×10^9	1.6×10^{12}
Spin-down luminosity $\dot{E}$ (erg/s)	5800×10^{30}	1.6×10^{30}
Mass function ($M_\odot$)	0.29097(1)	0.356(3)
Distance (kpc)	$\sim$0.6	
Total system mass $m_A + m_B$ ($M_\odot$)	2.588(3)	
Mass ratio $R \equiv m_A/m_B$	1.069(6)	
Orbital inclination from Shapiro s (deg)	87(3)	
Orbital inclination from $(R, \dot{\omega})$ (deg)	$87.7(-29, +17)$	
Stellar mass from $(R, \dot{\omega})$ ($M_\odot$)	1.337(5)	1.250(5)

Checking General Gelativity

The observational constraints upon the masses *m*A and *m*B. The colored regions are those which are excluded by the Keplerian mass functions of the two pulsars. Further constraints are shown as pairs of lines enclosing permitted regions as predicted by general relativity: (a) the measurement of the advance of periastron $\dot{\omega}$, giving the total mass *m*A+*m*B = 2:588 pm 0:003M (Sun) (dashed line); (b) the measurement of *R* = *m*A/*m*B = 1:069 pm 0:006 (solid line); (c) the measurement of the gravitational redshift/time dilation parameter (dot-dash line); (d) the measurement of Shapiro parameter *r* giving *m*B = 1:2 pm 0.3M (Sun) (dot-dot-dot-dash line) and (e) Shapiro parameter *s* (dotted line).

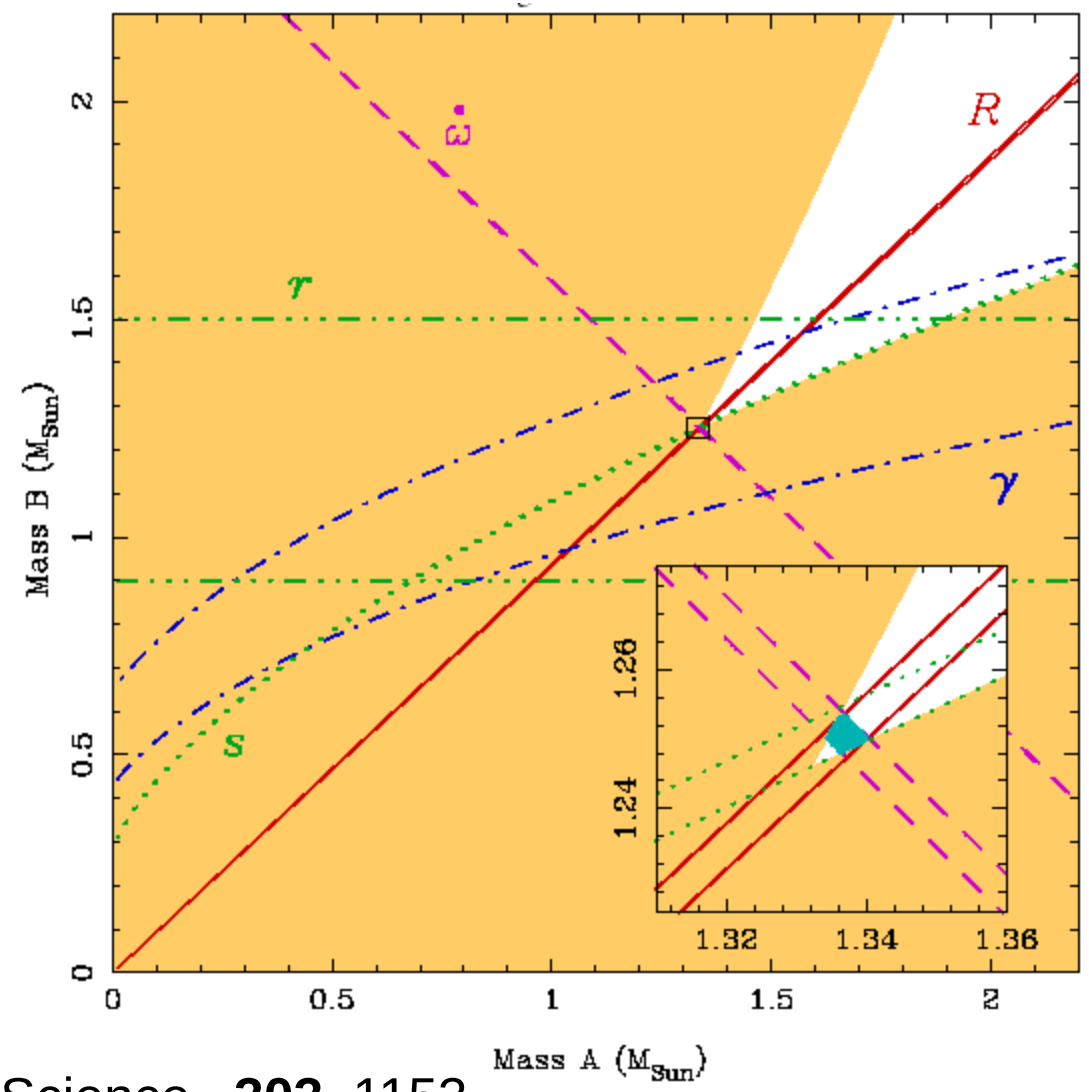

Lyne et al., 2004, Science, **303**, 1153.

TABLE I: Observed and derived parameters of PSRs J0737−3039A and B. Standard errors are given in parentheses after the values and are in units of the least significant digit(s).

Pulsar	PSR J0737−3039A	PSR J0737−3039B
Pulse period P (ms)	22.699378556138(2)	2773.4607474(4)
Period derivative $\dot{P}$	$1.7596(2) \times 10^{-18}$	$0.88(13) \times 10^{-15}$
Epoch of period (MJD)	52870.0	
Right ascension α (J2000)	$07^{\rm h}37^{\rm m}51^{\rm s}.24795(2)$	
Declination δ (J2000)	$-30^\circ 39' 40''.7247(6)$	
Orbital period $P_{\rm b}$ (day)	0.1022515628(2)	
Eccentricity e	0.087778(2)	
Epoch of periastron T_0 (MJD)	52870.0120588(3)	
Advance of periastron $\dot{\omega}$ (deg yr^{-1})	16.900(2)	
Longitude of periastron ω (deg)	73.805(1)	73.805 + 180.0
Projected semi-major axis $x = a\sin i/c$ (sec)	1.415032(2)	1.513(4)
Gravitational redshift parameter γ (ms)	0.39(2)	
Shapiro delay parameter $s = \sin i$	0.9995(4)	
Shapiro delay parameter r (μs)	6.2(6)	
Orbital decay $\dot{P}_{\rm b}$ (10^{-12})	−1.20(8)	
Mass ratio $R = M_A/M_B$	1.071(1)	

M.~Kramer et al., astro-ph/0503386.

The observational constraints upon the masses *m*A and *m*B. The colored regions are those which are excluded by the Keplerian mass functions of the two pulsars. Further constraints are shown as pairs of lines enclosing permitted regions as predicted by general relativity: (a) the measurement of the advance of periastron , giving the total mass *m*A+*m*B = 2.588 pm 0.003M (Sun) (dashed line); (b) the measurement of *R* = *m*A/*m*B = 1.069 pm 0.006 (solid line); (c) the measurement of the gravitational redshift/time dilation parameter (dot-dash line); (d) the measurement of Shapiro parameter *r* giving *m*B = 1.2 pm 0.3M (Sun) (dot-dot-dot-dash line) and (e) Shapiro parameter *s* (dotted line).

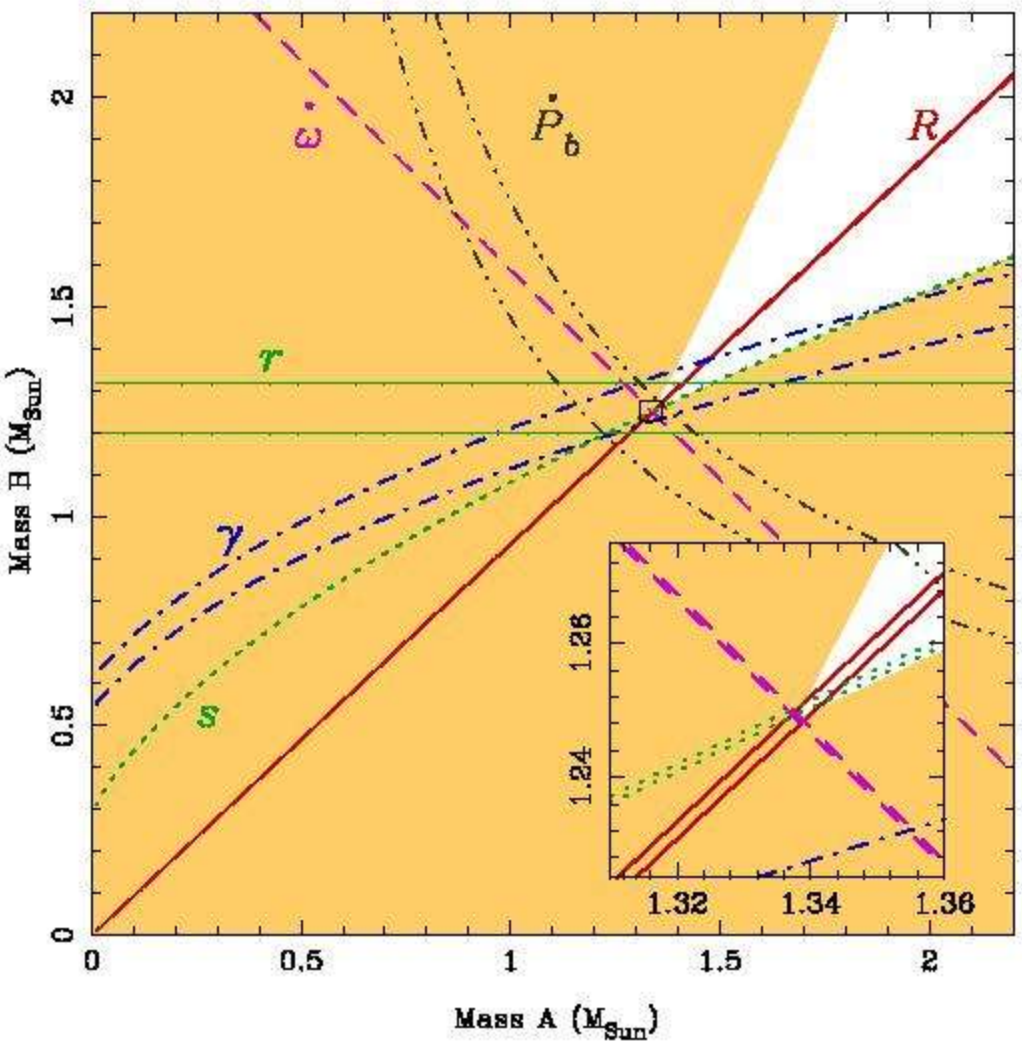

M. Kramer et al., astro-ph/0503386.

Past and Future of PSR J0737-3039A,B

$$\frac{dA}{dt} = -\frac{64}{5}\frac{m_1 m_2 (m_1+m_2)}{a^3(1-e^2)^{7/2}} \times \left(1+\frac{73}{24}e^2+\frac{37}{96}e^4\right)$$

$$\frac{de}{dt} = -\frac{304}{15}\frac{m_1 m_2 (m_1+m_2) e}{A^4(1-e^2)^{5/2}} \left(1+\frac{121}{304}e^2\right)$$

$$m_1 = 1.34\, M_\odot (\text{millisecond pulsar}),$$
$$m_2 = 1.25\, M_\odot, \quad e_0 = 0.0878,$$
$$P_{b0} = 0.102 \text{ days} = 8.83 \times 10^3 \text{ s},$$
$$A_0 = 8.8 \times 10^{10} \text{ cm}.$$

MPA, 11 April, 2006

G. S. Bisnovaty -Kogan
and
A . V. Tutukov

Astronomicheski.. Zhurnal,
Vol. 81, No. 9, 2004, p. 797.

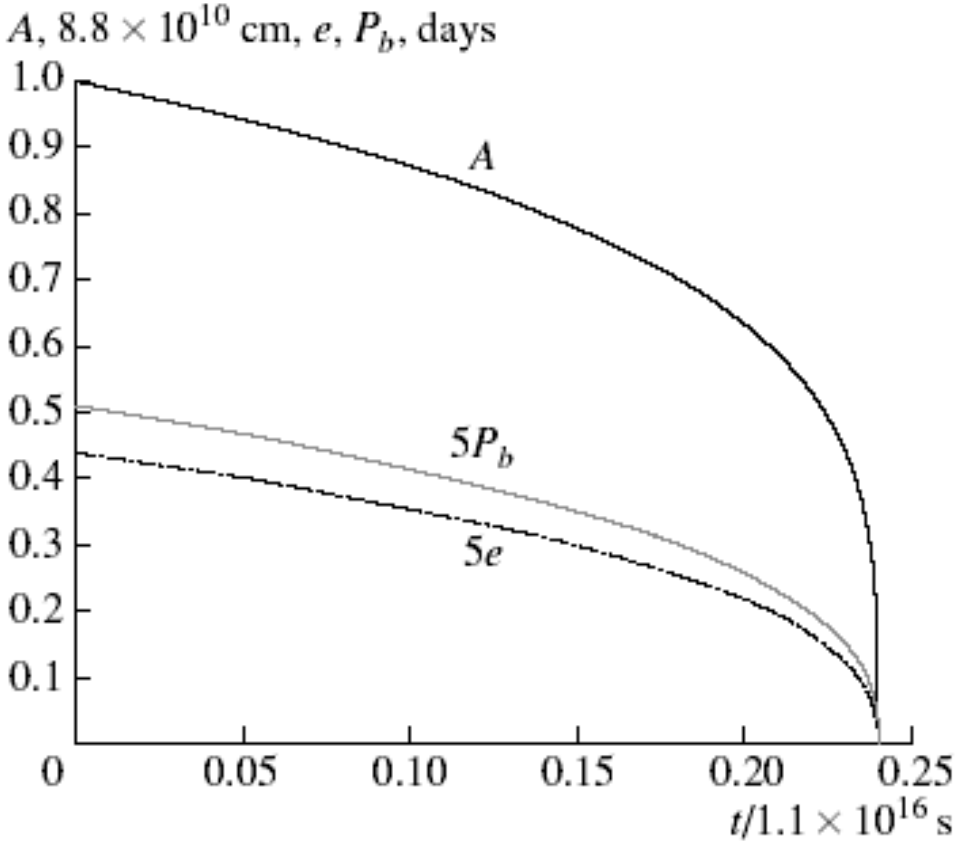

Fig. 1. Evolution of the semimajor axis A, orbital period P_b, and eccentricity e of the binary system due to the action of gravitational radiation.

MPA, 11 April, 2006

G. S. Bisnovaty - Kogan

and

A . V. Tutukov

Astronomicheski.. Zhurnal,

Vol. 81, No. 9, 2004, p. 797.

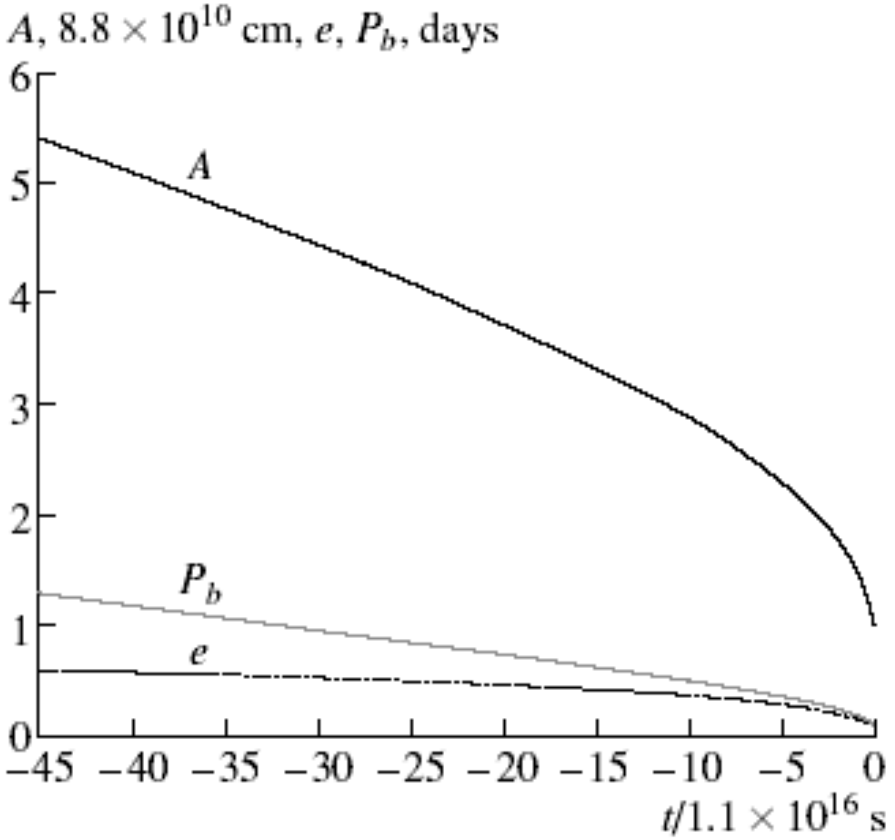

Fig. 2. Possible past evolution of the semimajor axis A, orbital period P_b, and eccentricity e of the binary system due to the action of gravitational radiation.

MPA, 11 April, 2006

Variability of the gravitational constant.

A. Paleontological and geophysical arguments

1. Earth surface temperature $|\dot{G}/G| < 2.0 \times 10^{-11}\ \mathrm{yr}^{-1}$

2. Expanding Earth $-\dot{G}/G \lesssim 8 \times 10^{-12}\ \mathrm{yr}^{-1}.$

B. Planetary and stellar orbits

$$\frac{\dot{P}}{P} = -2\frac{\dot{G}}{G}.$$

1. Early works Moon eclipces (example)

1374 B.C. to 1715 A.D. $\dot{G}/G = (2.6 \pm 15) \times 10^{-11}\ \mathrm{yr}^{-1}.$

2. Solar system

$$\dot{G}/G = (0.0 \pm 2.0) \times 10^{-12}\ \mathrm{yr}^{-1}.$$

Variability of the gravitational constant.

The Lunar Laser Ranging (LLR) experiment has measured the position of the Moon with an accuracy of about 1 cm for 30 years.

from the first six years of LLR $|\dot{G}/G| \lesssim 3 \times 10^{-11}\ \mathrm{yr}^{-1}$.

20 years of data to improve this result to $|\dot{G}/G| < 1.04 \times 10^{-11}\ \mathrm{yr}^{-1}$

the main error arising from the Lunar tidal acceleration.

24 years of data concluded that $|\dot{G}/G| < 6 \times 10^{-12}\ \mathrm{yr}^{-1}$,

J. O. Dickey *et al.*, Science **265**, 482 (1994).

Using all available astrometric data and in particular the ranging data from Viking landers on Mars $|\dot{G}/G| = (2 \pm 4) \times 10^{-12}\ \mathrm{yr}^{-1}$.

Hellings et al., Phys. Rev. Lett. 51 (1983) 1609

Stellar constraints

Solar evolution in the presence of a time-varying gravitational constant.

$$|\dot{G}/G| < 1.6 \times 10^{-12}\ \mathrm{yr}^{-1}$$

Variability of the gravitational constant.

Binary Recycled Pulsars

1. T.Damour, G.Gibbons, J.Taylor, PRL, **61,** 1151 (1988)

Limits on the Variability of G Using Binary-Pulsar Data

One of the few experimental handles on unified theories of gravity with other interactions comes from possible time variation of coupling constants over the Hubble time: $H_0^{-1} \simeq (7.67 \times 10^{-11}\ \mathrm{yr}^{-1})^{-1}$. We present a new theory-independent estimate (consistent with zero) of the time variation of Newton's gravitational constant derived from the timing of the binary pulsar PSR 1913+16: $\dot{G}_0/G_0 = (1.0 \pm 2.3) \times 10^{-11}\ \mathrm{yr}^{-1}$. We anticipate that this estimate will become sharper as more data are acquired.

After complicated calculations: $\dot{P}_0^{\mathrm{tot}} = \dot{P}_0^{\mathrm{GR}} - 2P_0\dot{G}_0/G_0.$

2. ApJ, **428,** 713 (1994)

HIGH-PRECISION TIMING OF MILLISECOND PULSARS. III. LONG-TERM MONITORING OF PSRs B1885+09 AND B1937+21

V. M. KASPI,[1] J. H. TAYLOR,[2] AND M. F. RYBA[3]

$$\frac{\dot{G}}{G} = (4 \pm 5) \times 10^{-12}\ \mathrm{yr}^{-1} \quad (\mathrm{PSR\ B1913+16})$$

$$\frac{\dot{G}}{G} = (-9 \pm 18) \times 10^{-12}\ \mathrm{yr}^{-1} \quad (\mathrm{PSR\ B1855+09})\ .$$

Checking the variability of the gravitational constant with binary pulsars

PSR B1913+16

Table 1: Error budget for the orbital period derivative, in comparison with the general relativistic prediction, from [10].

	Parameter	(10^{-12})
Observed value	$\dot{P}_b^{obs}$	-2.4225±0.0056
Galactic contribution	$\dot{P}_b^{gal}$	-0.0124±0.0064
Intrinsic orbital period decay	$\dot{P}_b^{obs}$ - $\dot{P}_b^{gal}$	-2.4101±0.0085
General relativistic prediction	$\dot{P}_b^{GR}$	-2.4025±0.0001

J.H. Taylor, Classical and Quantum Gravity 10 (1993) 167.

$$\frac{\dot{G}}{G} = -\frac{1}{2}\frac{\dot{P}_b}{P_b}, \quad \frac{\delta e}{e} = 0, \; e = \text{comst.}$$

Bisnovatyi-Kogan, gr-qc/0511072

RP PSR B1913+16 (1992)

$$\frac{\dot{G}}{G} = (4.3 \pm 4.9) \cdot 10^{-12}\,\text{yr}^{-1}.$$

better precision is expected from timing of **RP J0737-3039A**

The combination of Mariner 10 and Mercury and Venus ranging data gave (1992)

$$\dot{G}/G = (0 \pm 2) \cdot 10^{-12} \mathrm{yr}^{-1}$$

Combining with binary pulsar data we obtain

Bisnovatyi-Kogan, gr-qc/0511072

$$\dot{G}/G \text{ inside the limits } (-0.6 \div +2) \cdot 10^{-12} \text{ year}^{-1}$$

Recent results

Lunar Laser Ranging Tests of Relativistic Gravity

Williams et al. gr-qc/0411113

$$\dot{G}/G = (4 \pm 9) \times 10^{-13} \ \ \mathrm{yr}^{-1}$$

Lunar Laser Ranging Contributions to Relativity and Geodesy

J. Mueller, J. G. Williams, S. G. Turyshev **gr-qc/0509114**

Time varying gravitational constant $\dot{G}/G$ [yr^{-1}]	$(6 \pm 8) \cdot 10^{-13}$

GR improving the accuracy to $\sim 0.05\%$

Incompletely modeled solid Earth tides, ocean loading or geocenter motion, and uncertainties in values of fixed model parameters have to be considered in those estimations.

CONCLUSIONS

1. Timing of the pulsars J0737-3039A /B is the most poweful instrument for the verification of General Relativity due to unpresedented precision of the observations

2. Recycled pulsars are the most precise available time standards

3. Checking the physics beyond the standard: G-variability